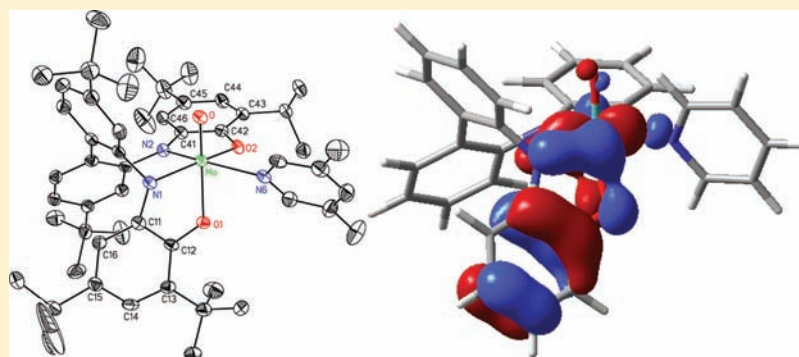


Molybdenum(VI) Complexes of a 2,2'-Biphenyl-bridged Bis(amidophenoxide): Competition between Metal–Ligand and Metal–Amidophenoxide π Bonding

Jason A. Kopec, Sukesh Shekar, and Seth N. Brown*

Department of Chemistry and Biochemistry, 251 Nieuwland Science Hall, University of Notre Dame, Notre Dame, Indiana 46556-5670, United States

S Supporting Information



ABSTRACT: The 2,2'-biphenyl-bridged bis(2-aminophenol) ligand 4,4'-di-*tert*-butyl-*N,N'*-bis(3,5-di-*tert*-butyl-2-hydroxyphenyl)-2,2'-diaminobiphenyl (${}^t\text{BuClipH}_4$) reacts with $\text{MoO}_2(\text{acac})_2$ to form $({}^t\text{BuClipH}_2)\text{MoO}_2$, where the diarylamines remain protonated and bind trans to the terminal oxo groups. This complex readily loses water on treatment with pyridine or 3,5-lutidine to form mono-oxo complexes $({}^t\text{BuClip})\text{MoO}(\text{L})$, which exhibit predominantly a *cis*- β geometry with an aryloxide trans to the oxo group. Exchange of the pyridine ligands is rapid and takes place by a dissociative mechanism, which occurs with retention of stereochemistry at molybdenum. Oxo-free alkoxide complexes $({}^t\text{BuClip})\text{Mo}(\text{OR})_2$ are formed from $({}^t\text{BuClipH}_2)\text{MoO}_2$ and ROH. Treatment of $\text{NMo}(\text{O}^t\text{Bu})_3$ with ${}^t\text{BuClipH}_4$ results in complete deprotonation of the bis(aminophenol) and formation of a dimolybdenum complex $({}^t\text{BuClip})\text{Mo}(\mu\text{-N})(\mu\text{-NH}_2)\text{Mo}({}^t\text{BuClip})$ containing both a bridging nitride ($\text{Mo-N} = 1.848 \text{ \AA}$, $\text{Mo-N-Mo} = 109.49^\circ$) and a bridging amide group. The strong π bonding of this bis(amidophenoxide) ligand allows the molybdenum center to interconvert readily among species forming three, two, one, or zero π bonds from multiply bonded ligands.

INTRODUCTION

The chemistry of molybdenum(VI) is dominated by oxo ligands, and to a lesser extent other strong π -donors such as imido, nitrido, alkylidene, and alkylidyne ligands. The $\text{Mo}=\text{O}$ homolytic bond dissociation energy is among the highest known.¹ While loss of a single oxo from a dioxomolybdenum complex is often observed, complete deoxygenation of oxomolybdenum complexes is rare, and indeed molybdenum(VI) compounds devoid of metal–ligand multiple bonds are uncommon regardless of their synthetic provenance.² The propensity of high-valent molybdenum to form metal–ligand multiple bonds stems from the metal's high Lewis acidity and its d^0 configuration. Multiply bonded ligands are required to achieve high valence electron counts while maintaining modest coordination numbers.

One exception to the hegemony of oxo and related ligands in the chemistry of molybdenum(VI) is provided by catecholates. Catecholates can be considered as isolobal to oxo, with the two σ bonds of the bidentate ligands paralleling the σ and one of the π bonds of the oxo ligand (Figure 1). The second π interaction of the oxo is analogous to donation from the B_1 -symmetric

donor orbital of the catecholate, which is raised in energy by its interaction with a filled benzene π -bonding orbital (the out-of-phase combination is lowered in energy because of its overlap with the benzene π^* orbital and is not an effective π donor).³

Congruent with the oxo/catecholate analogy, a variety of molybdenum(VI) tris(catecholates) are known,⁴ and mixed oxo-catecholate complexes are also common.^{5–7} In some cases, catecholate spectator ligands appear to enable the complete loss of ancillary terminal oxo ligands, which would otherwise be difficult to achieve at Mo(VI). For example, oxobis(3,6-di-*tert*-butylcatecholato)molybdenum(VI) is isolated as a tetramer with bridging rather than terminal oxo groups, and the oxo groups are lost entirely on reaction with isopropanol to give $(3,6\text{-}{}^t\text{Bu}_2\text{C}_6\text{H}_2\text{O}_2)_2\text{Mo}(\text{O}^i\text{Pr})_2$.⁶

Here we describe the preparation, characterization, and reactivity of molybdenum complexes of a tetradentate bis-(amidophenoxide) ligand. 2-Amidophenoxides are isoelectronic

Received: August 9, 2011

Published: January 19, 2012

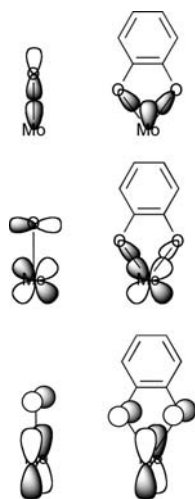


Figure 1. Bonding interactions in transition metal oxo (left) and catecholate (right) complexes.

with catecholates but are expected to be stronger π donors because of the greater basicity of nitrogen compared to oxygen.⁸ In the complexes reported here, the amidophenolate ligand can act as an oxo surrogate, and rapid dissociation of neutral ligands suggests that it is indeed a stronger donor than catecholate. Isolation of compounds with two, one, or zero other multiply bonded ligands also attests to the ability of the 2-amidophenoxides to stabilize high-valent molybdenum.

EXPERIMENTAL SECTION

Unless otherwise noted, all procedures were carried out under an inert atmosphere in a nitrogen-filled glovebox or on a vacuum line. When dry solvents were needed, chlorinated solvents and acetonitrile were dried over 4 Å molecular sieves, followed by CaH_2 . Benzene and toluene were dried over sodium, and ether and tetrahydrofuran over sodium benzophenone ketyl. Alcohols were dried over 4 Å molecular sieves. Deuterated solvents were obtained from Cambridge Isotope Laboratories, dried using the same procedures as their protio analogues, and stored in the drybox prior to use. 2,2'-Diamino-4,4'-di-*tert*-butylbiphenyl was prepared in two steps from 4,4'-di-*tert*-butylbiphenyl (Aldrich or Alfa-Aesar) as described by Tashiro and Yamato.⁹ Nitridotri(*tert*-butoxy)molybdenum(VI) was prepared from $\text{MoCl}_4(\text{CH}_3\text{CN})_2$ and was purified by sublimation.¹⁰ All other reagents were commercially available and used without further purification. Routine NMR spectra were measured on a Varian VXR-300 or Bruker DPX-400 spectrometer. Chemical shifts for ^1H and $^{13}\text{C}\{^1\text{H}\}$ spectra are reported in parts per million (ppm) downfield of TMS, with spectra referenced using the known chemical shifts of the solvent residuals. Infrared spectra were recorded as nujol mulls between NaCl plates on a Thermo Nicolet Nexus 470 ESP FT-IR spectrometer. Electrospray ionization (ESI) mass spectra were obtained using a Bruker micrOTOF-II mass spectrometer, and peaks reported are the mass number of the most intense peak of isotope envelopes. Samples were injected as dichloromethane solutions, preceded and followed by methanol. In all cases, the observed isotope patterns were in good agreement with calculated ones. UV–visible spectra were measured using dichloromethane solutions in 1-cm quartz cuvettes with a Beckman DU-7500 diode array spectrophotometer. Elemental analyses were performed by M–H–W Laboratories (Phoenix, AZ) or Midwest Microlab, LLC (Indianapolis, IN).

4,4'-Di-*tert*-butylbiphenyl-2,2'-bis((2-hydroxy-3,5-di-*tert*-butylphenyl)amine), $^t\text{BuClipH}_4$. Into a 50 mL Erlenmeyer flask in the air were weighed 0.5085 g of 2,2'-diamino-4,4'-di-*tert*-butylbiphenyl (1.715 mmol) and 0.7703 g of 3,5-di-*tert*-butylcatechol (Aldrich, 2.02 equiv). Hexane (15 mL) and a magnetic stirbar were added to the flask. Triethylamine (25 μL) was added to the vigorously stirred suspension. Within about 15 min, the suspension darkened and turned

brown. The flask was sealed with parafilm and stirring was continued overnight. After 24 h, the mixture was filtered and the pasty white solid isolated by suction filtration on a glass frit, washed with 2×5 mL hexane, and air-dried 15 min to furnish 0.9688 g of $^t\text{BuClipH}_4$ (80%). ^1H NMR (CDCl_3): δ 1.24 (s, 36H, $2 \times ^t\text{Bu}$), 1.43 (s, 18H, ^tBu), 5.13 (sl br s, 2H, NH), 6.24 (s, 2H, OH), 6.68 (d, 2 Hz, H-3), 6.99 (dd, 8, 2 Hz, 2H, H-5), 7.01 (d, 2.5 Hz, 2H, ArH), 7.17 (d, 2.5 Hz, 2H, ArH), 7.25 (d, 8 Hz, 2H, H-6). $^{13}\text{C}\{^1\text{H}\}$ NMR (CDCl_3): δ 29.69, 31.42, 31.79 ($\text{C}(\text{CH}_3)_3$), 34.56, 34.95, 35.17 ($\text{C}(\text{CH}_3)_3$), 111.91, 117.34, 121.23, 121.65, 122.53, 128.13, 130.83, 135.57, 142.46, 144.32, 149.04, 152.67. IR: 3534 (w), 3440 (s), 3403 (m), 3346 (m), 3321 (m), 1601 (m), 1564 (s), 1478 (s), 1413 (s), 1307 (s), 1221 (s), 1192 (s), 1160 (w), 1135 (w), 1111 (m), 1029 (m), 1004 (m), 980 (m), 947 (m), 763 (m), 722 (w), 690 (w), 645 (w). ESI-MS: 705.5405 ($\text{M}+\text{H}^+$), calcd 705.5359. Anal. Calcd for $\text{C}_{48}\text{H}_{68}\text{N}_2\text{O}_2$: C, 81.77; H, 9.72; N, 3.97. Found: C, 81.53; H, 9.83; N, 3.71.

Dioxo(4,4'-Di-*tert*-butylbiphenyl-2,2'-bis((2-oxy-3,5-di-*tert*-butylphenyl)amino)-molybdenum(VI), $(^t\text{BuClipH}_2)\text{MoO}_2$. Dioxo-molybdenum bis(acetylacetonate) (Strem, 0.4586 g; 1.41 mmol) and $^t\text{BuClipH}_4$ (0.9904 g, 1.40 mmol) were dissolved in chloroform (15 mL). The solution rapidly turned dark purple. The bright yellow precipitate that formed over 72 h was collected by filtration and washed with 2×10 mL of hexane to yield 0.8397 g of $(^t\text{BuClipH}_2)\text{MoO}_2$ (72%). ^1H NMR (CDCl_3): δ 1.05, 1.24, 1.27 (s, 18H each, ^tBu), 6.30 (dd, 2.2, 0.7 Hz, 2H, ArH), 6.47 (d, 8.0 Hz, 2H, H-6), 6.69 (sl br s, 2H, NH), 6.84 (d, 2.4 Hz, 2H, ArH), 6.87 (dd, 8.0, 1.7 Hz, 2H, H-5), 7.02 (d, 2.0 Hz, H-3). The compound was not sufficiently soluble for $^{13}\text{C}\{^1\text{H}\}$ NMR spectroscopic analysis. IR (nujol mull, cm^{-1}): 3216 (s, ν_{NH}), 1361 (s), 1305 (m), 1270 (m), 1255 (m), 1234 (w), 1202 (w), 1167 (w), 1115 (w), 1000 (w), 968 (w), 935 (s, ν_{MoO_2}), 900 (s, ν_{MoO_2}), 875 (s), 853 (m), 834 (m), 820 (m), 804 (w), 765 (m), 758 (m), 746 (m), 715 (w). ESI-MS: 829.4256 ($(^t\text{BuClip})\text{Mo}(\text{OCH}_3)^+$, calcd 829.4212), 815.4076 ($\text{M}^+ - \text{OH}$, calcd 815.4055). Anal. Calcd for $\text{C}_{48}\text{H}_{66}\text{MoN}_2\text{O}_4$: C, 69.38; H, 8.01; N, 3.37. Found: C, 69.19; H, 7.89; N, 3.25.

(μ -Nitrido)(μ -amido)bis(4,4'-Di-*tert*-butylbiphenyl-2,2'-bis((2-oxy-3,5-di-*tert*-butylphenyl)amido)dimolybdenum(VI), $(^t\text{BuClip})\text{Mo}(\mu\text{-N})(\mu\text{-NH}_2)\text{Mo}(^t\text{BuClip})$. $\text{NMo}(\text{O}^t\text{Bu})_3$ (0.3447 g, 1.05 mmol) and $^t\text{BuClipH}_4$ (0.7385 g, 1.05 mmol) were dissolved in 50 mL of ether and allowed to stir for 3 h. After 3 d standing at room temperature (RT), a violet precipitate had formed. It was suction filtered to yield 458 mg (54%) of the bridging nitride complex. ^1H NMR (CDCl_3): δ 0.68, 0.99, 1.03, 1.05, 1.09, 1.40 (s, 18H each, ^tBu), 4.69 (s, 2H, NH_2), 5.63 (d, 2 Hz, 2H, ArH), 5.94 (d, 2 Hz, 2H, ArH), 6.55 (d, 2 Hz, 2H, H-3), 6.61 (d, 2 Hz, 2H, ArH), 6.72 (d, 2 Hz, 2H, ArH), 6.77 (dd, 8, 2 Hz, 2H, H-5), 6.93 (d, 8 Hz, 2H, H-6), 7.02 (dd, 8, 2 Hz, 2H, H-5), 7.14 (d, 8 Hz, 2H, H-6), 7.17 (d, 2 Hz, 2H, H-3). $^{13}\text{C}\{^1\text{H}\}$ NMR (CDCl_3): δ 29.67, 29.89, 31.20, 31.31, 31.77, 31.96 ($\text{C}(\text{CH}_3)_3$), 34.43, 34.57, 34.58, 34.62, 34.68, 34.88 ($\text{C}(\text{CH}_3)_3$), 111.74, 111.89, 118.10, 120.04, 120.53, 122.15, 123.43, 123.49, 126.59, 129.16, 131.46, 132.35, 134.34, 134.72, 140.41, 142.93, 143.12, 145.40, 148.64, 149.26, 151.45, 153.28, 159.49, 165.16. IR: 3395 (m, ν_{NH}), 3305 (m, ν_{NH}), 1377 (s), 1360 (s), 1304 (m), 1258 (w), 1234 (w), 1199 (m), 1169 (m), 1131(w), 1021 (w), 992 (w), 947 (w), 931 (w), 910 (m), 853 (m), 833 (m), 812 (m), 780 (w), 767 (w), 743 (w), 722 (w), 702 (w), 647 (s), 620 (m), 592 (m). ESI-MS: $m/z = 1624.8271$ (M^+ , calcd 1624.8292). Anal. Calcd for $\text{C}_{96}\text{H}_{130}\text{Mo}_2\text{N}_6\text{O}_4$: C, 71.00; H, 8.07; N, 5.17. Found: C, 70.05; H, 7.40; N, 4.76.

$(^t\text{BuClip})\text{MoO}(\text{py})$. A solution of $(^t\text{BuClipH}_2)\text{MoO}_2$ (0.0505 g, 0.0608 mmol) and pyridine (9.7 μL , 0.12 mmol, 2.0 equiv) in benzene (2.5 mL) was stirred for 72 h under N_2 . The solvent was evaporated in vacuo to give a dark green powder. The product was dissolved in 1 mL of CH_3CN containing a drop of pyridine and placed in a -35 °C freezer for 1 week. The fine black crystals were filtered to yield 0.0224 g (41%) of $(^t\text{BuClip})\text{MoO}(\text{py})$. ^1H NMR (CDCl_3): δ 1.03, 1.07, 1.12, 1.18, 1.39, 1.41 (s, 9H ea., ^tBu), 5.88 (d, 2 Hz, 1H, ArH), 6.24 (d, 2 Hz, 1H, ArH), 6.69 (d, 2.5 Hz, 1H, ArH), 6.74 (d, 2 Hz, 1H, ArH), 6.77 (dd, 8, 2 Hz, 1H, H-5), 6.90 (d, 8 Hz, 1H, H-6), 6.91 (d, 1.5 Hz, 1H, H-3), 7.42 (dd, 8, 2 Hz, 1H, H-5), 7.47 (d, 8 Hz, 1H, H-6), 7.52 (br, 2H, py 3,5-H), 7.55 (d, 2 Hz, 1H, H-3), 7.92 (br, 1H, py 4-H), 9.09 (br, 2H, py 2,6-H). $^{13}\text{C}\{^1\text{H}\}$ NMR (CDCl_3): δ 29.52, 29.87,

31.34, 31.49, 31.58, 31.93 (C(CH₃)₃), 34.36, 34.51, 34.54, 34.64, 34.75, 35.08 (C(CH₃)₃), 111.64, 112.59, 116.17, 118.48, 120.51, 123.81, 124.87, 125.12, 125.23, 127.97, 129.30, 131.20, 131.72, 134.05, 135.82, 139.43, 141.25, 143.09, 146.06, 146.36, 150.21, 150.37 (2C), 150.80, 151.79, 155.71, 161.83. IR (cm⁻¹): 1606 (m), 1410 (m), 1363 (s), 1240 (s), 1218 (s), 1201 (w), 1071 (m), 1044 (m), 1017 (w), 993 (w), 959 (m), 940 (w), 901 (vs, $\nu_{\text{Mo=O}}$), 860 (w), 816 (s), 760 (s), 727 (w), 695 (m), 659 (w). UV-vis (CH₂Cl₂) λ_{max} 320 nm ($\epsilon = 24700 \text{ M}^{-1} \text{ cm}^{-1}$), 445 (13900), 586 (10700). Anal. Calcd for C₅₃H₆₉N₃O₃Mo: C, 71.36; H, 7.80; N, 4.71. Found: C, 71.33; H, 8.05; N, 4.70.

(^tBuClip)MoO(3,5-Me₂C₅H₃N). A solution of (^tBuClipH₂)MoO₂ (0.0514 g, 0.0619 mmol) and 3,5-lutidine (10.3 μL , 0.0903 mmol, 1.46 equiv) in benzene (2.5 mL) was stirred for 30 min under N₂ and the solvent then evaporated on a vacuum line. The black powder was dissolved in 0.5 mL of benzene containing a drop of 3,5-lutidine, layered with 3.5 mL of acetonitrile, and allowed to stand for 1 week. The fine black crystals formed were collected by filtration to give 0.0392 g of (^tBuClip)MoO(lut) (69%). ¹H NMR (CDCl₃): δ 1.03, 1.07, 1.12, 1.18, 1.40, 1.42 (s, 9H ea., ^tBu), 2.39 (s, 6H, lut CH₃), 5.88 (d, 2 Hz, 1H, ArH), 6.24 (d, 2 Hz, 1H, ArH), 6.68 (d, 2 Hz, 1H, ArH), 6.74 (d, 2 Hz, 1H, ArH), 6.76 (dd, 8, 2 Hz, 1H, H-5), 6.90 (d, 7.5 Hz, 1H, H-6), 6.90 (d, 2 Hz, 1H, 3-H), 7.41 (dd, 8.5 Hz, 2 Hz, 1H, H-5), 7.47 (d, 8 Hz, 1H, H-6), 7.52 (br, 1H, lut 4-H), 7.55 (d, 1.5 Hz, 1H, H-3), 8.70 (br, 2H, lut 2,6-H). ¹³C{¹H} NMR (CDCl₃): δ 18.60 (lut CH₃), 29.46, 29.91, 31.37, 31.53, 31.60, 31.96 (C(CH₃)₃), 34.39, 34.52, 34.55, 34.68, 34.76, 35.09 (C(CH₃)₃), 111.67, 112.55, 115.93, 118.51, 120.48, 123.92, 125.01, 125.14, 127.98, 129.45, 131.31, 131.77, 133.95, 134.22, 135.82, 140.71, 141.16, 142.98, 146.18, 146.43, 147.84 (2C), 150.04, 150.15, 150.84, 151.74, 155.71. IR (cm⁻¹): 1601 (w), 1410 (m), 1361 (m), 1313 (w), 1282 (w), 1260 (w), 1241 (m), 1201 (w), 1174 (w), 1155 (m), 991 (w), 956 (w), 936 (w), 907 (vs, $\nu_{\text{Mo=O}}$), 814 (w), 770 (w), 753 (w), 742 (w), 699 (w). Anal. Calcd for C₅₅H₇₃N₃O₃Mo: C, 71.79; H, 8.00; N, 4.57. Found: C, 71.59; H, 8.20; N, 4.84.

(^tBuClip)Mo(OⁱPr)₂. (^tBuClip)Mo(μ -N)(μ -NH₂)Mo(^tBuClip) (166 mg, 0.181 mmol) was dissolved in 5 mL of chloroform. After adding 1 mL of dry isopropanol, the reaction mixture was stirred 25 h under N₂. The solvent was evaporated in vacuo to yield 168 mg of crude (^tBuClip)Mo(OⁱPr)₂, which was recrystallized from CH₂Cl₂ (2 mL) layered with acetonitrile (3 mL) to yield 45 mg (27%) of pure diisopropoxide. The analytical sample contained one equivalent of CH₂Cl₂. ¹H NMR (CDCl₃): δ 1.11 (s, 18H, ^tBu), 1.14 (s, 18H, ^tBu), 1.22 (d, 6 Hz, 6H, OCH(CH₃)(CH₃')), 1.34 (d, 6 Hz, 6H, OCH(CH₃)-(CH₃')), 1.35 (s, 18H, ^tBu), 5.59 (sept, 6 Hz, 2H, OCH(CH₃)₂), 5.80 (d, 2 Hz, 2H, ArH), 6.65 (d, 2 Hz, 2H, H-3), 6.72 (d, 2 Hz, 2H, ArH), 7.05 (dd, 8, 2 Hz, 2H, H-5), 7.10 (d, 8 Hz, 2H, H-6). ¹³C{¹H} NMR (CDCl₃): δ 24.73, 25.81 (OCH(CH₃)(CH₃')), 29.99, 31.31, 31.84 (C(CH₃)₃), 34.48, 34.73, 34.92 (C(CH₃)₃), 76.94 (OCH(CH₃)₂), 108.20, 120.00, 121.47, 123.58, 127.47, 130.95, 135.64, 144.42, 145.11, 149.96, 150.51, 156.75. IR: 3170 (w), 1605 (m), 1585 (m), 1556 (m), 1376 (s), 1364 (s), 1303 (m), 1256 (w), 1201 (m), 1166 (m), 1108 (s), 966 (s), 853 (s), 820 (s), 594 (s). ESI-MS: $m/z = 939.4880$ (M⁺+Na, calcd 939.4922). Anal. Calcd for C₅₃H₈₀Cl₂MoN₂O₄: C, 66.05; H, 8.06; N, 2.80. Found: C, 66.53; H, 8.13; N, 2.98.

(^tBuClip)Mo(OCH₃)₂. The methoxide complex was generated analogously by treatment of (^tBuClip)Mo(μ -N)(μ -NH₂)Mo(^tBuClip) with CH₃OH in chloroform; evaporation of the volatiles produced a dark purple oil. ¹H NMR (CDCl₃): δ 1.10, 1.15, 1.36 (s, 18H ea., ^tBu), 4.74 (s, 6H, OCH₃), 5.82 (d, 2 Hz, 2H, ArH), 6.64 (s, 2H, H-3), 6.71 (d, 2 Hz, 2H, ArH), 7.07 (m, 4H, H-5 and H-6). ¹³C{¹H} NMR (CDCl₃): δ 29.77, 31.20, 31.71 (C(CH₃)₃), 34.38, 34.57, 34.98 (C(CH₃)₃), 65.08 (OCH₃), 108.50, 120.74, 121.39, 123.82, 127.29, 130.89, 135.54, 143.45, 145.98, 150.01, 150.77, 156.79.

Electrochemistry. Electrochemical measurements were performed in the drybox using a BAS Epsilon potentiostat. A standard three-electrode setup was used, with a glassy carbon working electrode, Pt or glassy carbon counter electrode, and a silver/silver chloride pseudo-reference electrode. The electrodes were connected to the potentiostat through electrical conduits in the drybox wall. Samples were

approximately 1 mM in CH₂Cl₂, using 0.1 M Bu₄NPF₆ as the electrolyte. Potentials were referenced to ferrocene/ferrocenium at 0 V,¹¹ with the reference potential established by spiking the test solution with a small amount of ferrocene or decamethylferrocene ($E^\circ = -0.565 \text{ V}^{12}$). Cyclic voltammograms were recorded with a scan rate of 60 mV s⁻¹.

Calculations. Geometry optimizations and orbital calculations were performed on the model compounds (Clip)MoO(py) and (Clip)-Mo(μ -N)(μ -NH₂)Mo(Clip) where all six *tert*-butyl groups of ^tBuClip were replaced by hydrogen atoms. Calculations used the hybrid B3LYP method, with an SDD basis set for molybdenum and a 6-31G* basis set for all other atoms, using the Gaussian03 suite of programs.¹³ The molecular symmetry of (Clip)Mo(μ -N)(μ -NH₂)Mo(Clip) was constrained to be C₂ in the calculations. Optimized geometries were confirmed to be minima by frequency analysis. Plots of calculated Kohn–Sham orbitals were generated using the program GaussView (v. 5.0.8) with an isovalue of 0.04.

Variable-Temperature NMR Spectroscopy of (^tBuClip)MoO(L). NMR spectra were recorded between -50° and +50 °C in CDCl₃ on a Varian VXR-500 NMR spectrometer. The pyridine or lutidine resonances were simulated using the program gNMR¹⁴ to generate calculated lineshapes and superimpose them on the observed spectra. Activation parameters were calculated by plotting ln(k_{diss}/T) versus 1/T.

X-ray Crystallography. Crystals of (^tBuClip)Mo(μ -N)(μ -NH₂)-Mo(^tBuClip)-0.5Et₂O were grown by slow cooling of a concentrated solution of the complex in ether, while crystals of (^tBuClip)MoO(3,5-lut)-CH₃CN and (^tBuClip)Mo(OⁱPr)₂·2CH₃CN were grown by diffusion of acetonitrile into benzene solutions of the respective complexes. Crystals were placed in inert oil before transferring to the cold N₂ stream of a Bruker Apex II CCD diffractometer. Data were reduced, correcting for absorption, using the program SADABS. The structures were solved using direct methods, except for (^tBuClip)Mo(OⁱPr)₂·2CH₃CN, which was solved using a Patterson map. All nonhydrogen atoms not apparent from the initial solutions were found on difference Fourier maps, and all heavy atoms were refined anisotropically.

The ether in (^tBuClip)Mo(μ -N)(μ -NH₂)Mo(^tBuClip)-0.5Et₂O was disordered equally about the center of inversion, which was at the midpoint of a C–O bond. Two of the *tert*-butyl groups in this structure, those centered on C37 and C48, were disordered in two different orientations. All hydrogen atoms in (^tBuClip)Mo(μ -N)(μ -NH₂)Mo(^tBuClip)-0.5Et₂O and (^tBuClip)MoO(3,5-lut)-CH₃CN were placed in calculated positions, except the amido hydrogens in the former structure, which were found on difference Fourier maps and refined isotropically. Hydrogen atoms in (^tBuClip)Mo(OⁱPr)₂·2CH₃CN were found on difference Fourier maps and refined isotropically, except for solvent and *tert*-butyl hydrogens, which were placed in calculated positions. Calculations used SHELXTL (Bruker AXS),¹⁵ with scattering factors and anomalous dispersion terms taken from the literature.¹⁶ Further details about the individual structures are given in Table 1.

RESULTS

Preparation and Metalation of 4,4'-Di-*tert*-butyl-2,2'-bis((2-hydroxy-3,5-di-*tert*-butylphenyl)amino)biphenyl (^tBuClipH₄). Bis(aminophenol) ligands with 2,2'-biphenyl¹⁷ or 6,6'-dimethyl-2,2'-biphenyl¹⁸ backbones are known. Preparation of the 4,4'-di-*tert*-butyl-2,2'-biphenyl-bridged bis(aminophenol) ligand ^tBuClipH₄ proceeds analogously in three steps from commercially available 4,4'-di-*tert*-butylbiphenyl (Scheme 1). Nitration of the biphenyl and reduction of the dinitrobiphenyl are accomplished as described by Tashiro and Yamato,⁹ and base-catalyzed addition of the diamine to 3,5-di-*tert*-butylcatechol takes place in high yield to give the tetradentate ligand.

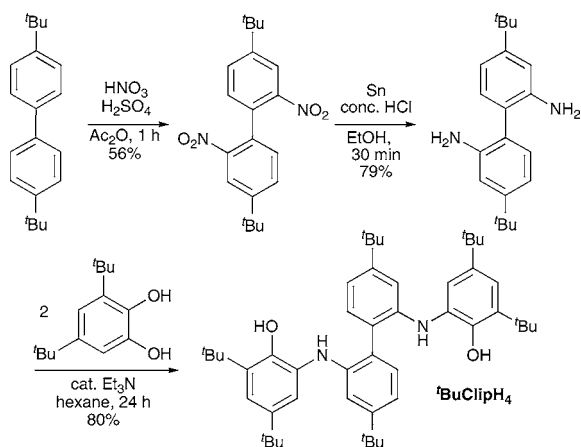
The bis(aminophenol) ligand ^tBuClipH₄ reacts with MoO₂-(*acac*)₂ in chlorinated solvents over the course of several days

Table 1. Crystal data for $({}^t\text{BuClip})_2\text{Mo}_2(\mu\text{-N})(\mu\text{-NH}_2)\cdot 0.5\text{Et}_2\text{O}$, $({}^t\text{BuClip})\text{MoO}(\text{Lut})\cdot\text{CH}_3\text{CN}$, and $({}^t\text{BuClip})\text{Mo}(\text{O}^i\text{Pr})_2\cdot 2\text{CH}_3\text{CN}$

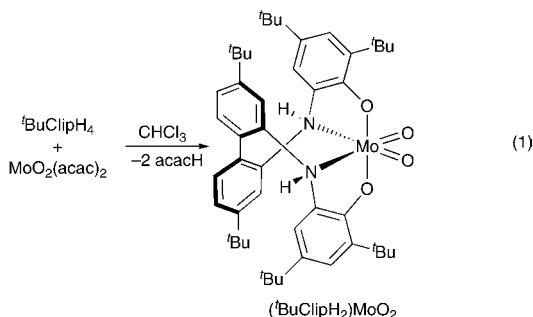
	$({}^t\text{BuClip})_2\text{Mo}_2(\mu\text{-N})(\mu\text{-NH}_2)\cdot 0.5\text{Et}_2\text{O}$	$({}^t\text{BuClip})\text{MoO}(\text{lut})\cdot\text{CH}_3\text{CN}$	$({}^t\text{BuClip})\text{Mo}(\text{O}^i\text{Pr})_2\cdot 2\text{CH}_3\text{CN}$
empirical formula	$\text{C}_{98}\text{H}_{135}\text{Mo}_2\text{N}_6\text{O}_{4.5}$	$\text{C}_{57}\text{H}_{76}\text{MoN}_4\text{O}_3$	$\text{C}_{58}\text{H}_{84}\text{MoN}_4\text{O}_4$
temperature (K)	100(2)	100(2)	120(2)
λ (Å)	1.54178 (Cu $K\alpha$)	1.54178 (Cu $K\alpha$)	0.71073 (Mo $K\alpha$)
space group	$P\bar{1}$	$Pna2_1$	$P\bar{1}$
total data collected	44466	50292	57132
no. of indep. refls.	15691	9975	9609
R_{int}	0.0275	0.0334	0.0285
obsd. refls. [$I > 2\sigma(I)$]	13443	9566	8706
a (Å)	14.7223(2)	22.5173(7)	13.8491(17)
b (Å)	15.4117(3)	12.1833(4)	14.7791(18)
c (Å)	21.2348(4)	19.6759(6)	14.9039(18)
α (deg)	88.7516(8)	90	72.332(3)
β (deg)	84.1354(8)	90	78.155(3)
γ (deg)	75.3810(7)	90	88.443(3)
V (Å ³)	4637.66(14)	5397.8(3)	2842.7(6)
Z	2	4	2
cryst size (mm)	$0.34 \times 0.25 \times 0.11$	$0.22 \times 0.17 \times 0.16$	$0.43 \times 0.35 \times 0.23$
no. refined params.	1028	589	918
R indices [$I > 2\sigma(I)$] ^a	$R1 = 0.0352$ $wR2 = 0.0898$	$R1 = 0.0322$ $wR2 = 0.0817$	$R1 = 0.0379$ $wR2 = 0.0949$
R indices (all data) ^a	$R1 = 0.0438$ $wR2 = 0.0953$	$R1 = 0.0339$ $wR2 = 0.0827$	$R1 = 0.0426$ $wR2 = 0.0988$
goodness of fit	1.017	1.052	1.050

$$^a R1 = \frac{\sum ||F_o| - |F_c||}{\sum |F_o|}; wR2 = \frac{[\sum [w(F_o^2 - F_c^2)^2]]}{\sum w(F_o^2)^2}^{1/2}.$$

Scheme 1. Preparation of the bis(2-aminophenol), ${}^t\text{BuClipH}_4$



to deposit sparingly soluble, bright yellow, microcrystalline $({}^t\text{BuClipH}_2)\text{MoO}_2$ (eq 1).



Free acetylacetonate is a byproduct of the reaction and can be observed in situ by ¹H NMR spectroscopy. The ¹H NMR

spectrum of the product is symmetrical, suggesting a *cis-α* geometry, and IR spectroscopy indicates the presence of stretches typical of a *cis*-dioxomolybdenum unit (935, 900 cm^{-1}) as well as an NH stretch at 3216 cm^{-1} . The NH protons resonate at δ 6.69 (CDCl_3), and couple weakly ($J = 0.5$ Hz) with the aminophenoxide aromatic peak at δ 6.30. A similar C_2 -symmetric, doubly deprotonated coordination mode has been observed in reactions of the analogous 1,2-phenylenediamine-bridged diphenol with $\text{Ti}(\text{OR})_4$ ($R = {}^i\text{Pr}, {}^t\text{Bu}$) or $\text{Zr}(\text{O}^t\text{Bu})_4$.¹⁹

Formation of a Bridging Nitrido Complex.

Nitridomolybdenum(VI) tris(*tert*-butoxide), $\text{NMo}(\text{O}^t\text{Bu})_3$, reacts with ${}^t\text{BuClipH}_4$ to release *tert*-butanol and form a diamagnetic purple compound with the empirical formula $({}^t\text{BuClipH})\text{MoN}$. Yields of this compound in situ are high as judged by NMR, but isolated yields are modest because of solubility losses. Its ¹H NMR spectrum reveals 10 aromatic resonances and 6 *tert*-butyl resonances due to a single, but unsymmetrical, environment of the ligand. A singlet at δ 4.69 is consistent with an NH proton, suggesting a monoprotonated ligand, as observed in an iron complex of the analogous 2,2'-biphenyl-bridged ligand.¹⁷ This structure is, however, ruled out by the observation of *two* NH stretches in the infrared spectrum (3305 and 3395 cm^{-1}), and a dimeric structure is suggested by the observation of a peak in the electrospray mass spectrum at double the mass expected for the empirical formula.

X-ray crystallography confirms the dimeric nature of the compound and indicates that it should be formulated as $({}^t\text{BuClip})\text{Mo}(\mu\text{-N})(\mu\text{-NH}_2)\text{Mo}({}^t\text{BuClip})$, with fully deprotonated bis(amidophenolate) ligands and a novel μ -nitrido/ μ -amido dimolybdenum core (Figure 2, Table 2). The amide and nitride groups are easily distinguished by their very different bond lengths to molybdenum, with the bridging nitride

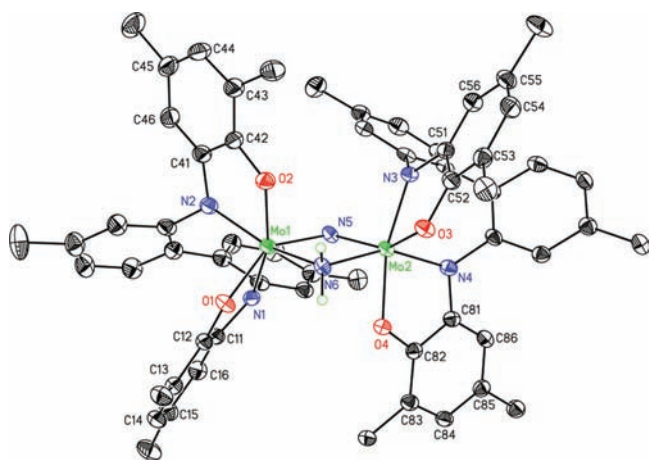


Figure 2. Thermal ellipsoid plot of $(t\text{BuClip})\text{Mo}(\mu\text{-N})(\mu\text{-NH}_2)\text{Mo}(t\text{BuClip})$. Hydrogen atoms (except those on N6), methyl groups, and lattice solvent have been omitted for clarity.

forming short bonds indicative of substantial multiple bonding ($\text{Mo}-\text{N}5 = 1.848(2) \text{ \AA}$ avg.) and the bridging amide forming much longer bonds ($\text{Mo}-\text{N}6 = 2.138(15) \text{ \AA}$ avg.); the two hydrogens on the bridging amide were also found on the difference Fourier map. The molecule has a (noncrystallographic) 2-fold axis passing through the nitride and amide nitrogens, relating the two molybdenum centers. While the geometry at molybdenum is approximately octahedral, there is substantial trigonal twisting (Table 2). The calculated twist angles²⁰ (0° for a perfect trigonal prism, 60° for a regular octahedron) of $35 \pm 11^\circ$ indicate a structure nearly midway between an octahedron and a trigonal prism (with the variability due to the irregularity of the coordination polyhedron). Similar trigonal distortions are seen in the oxocatecholates complexes $\text{MoO}(3,6\text{-}t\text{Bu}_2\text{C}_6\text{H}_2\text{O}_2)_2(\text{L})$ ($\text{L} = \text{C}_5\text{H}_5\text{NO}$, Me_2SO , Ph_3AsO).⁶

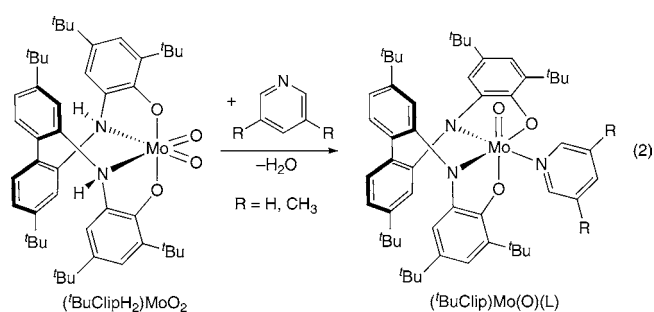
While bridging nitride complexes of molybdenum are common, the $\text{Mo}(\mu\text{-N})(\mu\text{-NH}_2)\text{Mo}$ structure has not been previously observed. The most common motif in molybdenum(VI) μ -nitrido complexes is a structure with alternating triple ($\sim 1.67 \text{ \AA}$) and single ($\sim 2.15 \text{ \AA}$) bonds, seen in tetramers of $\text{Mo}(\text{N})\text{Cl}_3$ ²¹ as well as in other structures.^{22,23} Lower-valent molybdenum species sometimes show substantial bond alternation,²⁴ but in other cases, more symmetrically bridged structures are observed.²⁵ Because the μ_2 -nitride is part of a four-membered ring, the $\text{Mo}-\text{N}-\text{Mo}$ angle of $109.49(10)^\circ$ is much more acute than any previously observed. Unconstrained bridging nitrides of molybdenum are invariably nearly linear, and even in known 6-membered ring nitrides the angles are greater than 144° .²³ While no structures with $\text{Mo}(\mu\text{-N})(\mu\text{-X})\text{Mo}$ cores have been reported previously, two bimetallic compounds with $\text{W}_2(\mu\text{-N})_2$ cores have been structurally characterized.²⁶ The tungsten nitrides also have acute $\text{W}-\text{N}-\text{W}$ angles ($\sim 95^\circ$), but show alternating single and multiple bonds to nitrogen. In contrast, the $\text{Mo}(\mu\text{-N})$ distances in $(t\text{BuClip})\text{Mo}(\mu\text{-N})(\mu\text{-NH}_2)\text{Mo}(t\text{BuClip})$ are symmetrical and are typical of molybdenum–nitrogen double bonds,²⁵ despite the fact that the bending at nitrogen allows formation of only one π bond and hence a $\text{Mo}-\text{N}$ bond order of only 1.5.

Despite the plethora of possible stereoisomers, only one is observed. It is not surprising that the axial chirality of the biphenyl is tightly coupled to the configuration at the metal,

as has been observed with biphenyl-bridged bis(salicylaldimines)²⁷ and bis(β -diketonates).²⁸ The observed *cis-β* configuration, uniquely among the three possible ways of wrapping the ligand around molybdenum, places an aryloxy (rather than amide) trans to the bridging nitride. In addition to placing the less basic donor trans to the nitride, consistent with the nitride's strong trans influence, this geometry maximizes the π overlap of the amido nitrogens with the lowest-lying Mo $d\pi$ orbitals, the ones of δ symmetry with respect to the bridging nitride (Supporting Information, Figure S1c–S1d). The relative configuration of the two molybdenum atoms could give a complex of overall C_2 or C_s symmetry, but the latter is excluded for steric reasons (the biphenyl bridges would be angled directly at one another).

Because of competition with π donation from the bridging nitride, the *cis* amidophenoxides donate less effectively to the molybdenum, and consequently their donor orbitals are modestly higher in energy ($\Delta E \approx 0.45 \text{ eV}$, Supporting Information, Figure S1). The cyclic voltammogram of $(t\text{BuClip})\text{Mo}(\mu\text{-N})(\mu\text{-NH}_2)\text{Mo}(t\text{BuClip})$ (Supporting Information, Figure S2a) shows one reversible ligand-centered oxidation at -0.03 V (vs $\text{Cp}_2\text{Fe}^+/\text{Cp}_2\text{Fe}$), but several other irreversible oxidations are perceptible between ~ 0.8 – 1.1 V . The complex also displays one reversible metal-centered reduction at -1.12 V .

Synthesis and Structure of Monooxo and Oxo-Free Molybdenum(VI) Complexes. In the solid state, $(t\text{BuClipH}_2)\text{MoO}_2$ is yellow, consistent with an octahedral dioxomolybdenum(VI) complex where all three $d\pi$ orbitals are $\text{Mo}=\text{O} \pi^*$ in character and thus high in energy, so the aryloxy-to-metal charge transfer bands are at short wavelength. Solutions of the complex quickly turn green, suggesting that the dioxo complex is in equilibrium with small amounts of species with fewer than two terminal oxo ligands, such as an oxo-hydroxo complex $(t\text{BuClipH})\text{MoO}(\text{OH})$ or oxo-aquo complex $(t\text{BuClip})\text{MoO}(\text{OH}_2)$. In the presence of Lewis bases such as pyridine or 3,5-lutidine, water is lost from the complex to give monooxo adducts $(t\text{BuClip})\text{MoO}(\text{L})$ in quantitative yield by NMR spectroscopy (eq 2).



Solid material can be obtained in moderate yields by crystallization from the reaction mixture in the presence of excess ligand, and infrared spectroscopy shows the absence of NH stretches and a single molybdenum-oxo stretch (901 cm^{-1} for the pyridine adduct, 907 cm^{-1} for the lutidine adduct). These frequencies are unusually low for monooxomolybdenum(VI) compounds, which typically absorb at about 940 cm^{-1} , but agree well with the scaled²⁹ value calculated by density functional theory (DFT) (911 cm^{-1} for $(\text{Clip})\text{MoO}(\text{py})$).

The solid-state structure of the 3,5-lutidine adduct $(t\text{BuClip})\text{MoO}(\text{lut})$ (Figure 3, Table 1) is very similar to that shown

Table 2. Selected Bond Distances (Å) and Angles (deg) for the First Coordination Spheres in (^tBuClip)MoO(lut)·CH₃CN, (^tBuClip)₂Mo₂(μ-N)(μ-NH₂)·0.5Et₂O, and (^tBuClip)Mo(OⁱPr)₂·2CH₃CN

	(^t BuClip)MoO(lut)·CH ₃ CN	(^t BuClip) ₂ Mo ₂ (μ-N)(μ-NH ₂)·0.5Et ₂ O		(^t BuClip)Mo(O ⁱ Pr) ₂ ·2CH ₃ CN
		Mo1 ^a	Mo2 ^{a,b}	
Mo–O1	2.0377(19)	2.0109(17)	2.0318(17)	2.0101(16)
Mo–O2	1.9730(18)	1.9800(17)	1.9825(17)	1.9937(16)
Mo–N1	2.046(2)	2.015(2)	2.013(2)	2.009(2)
Mo–N2	2.032(2)	2.035(2)	2.028(2)	2.0284(19)
Mo–O	1.7098(19)	1.847(2)	1.848(2)	
Mo–N6	2.253(2)	2.148(2)	2.127(2)	
Mo–O5				1.8865(16)
Mo–O6				1.9028(16)
O1–Mo–N1	74.36(9)	74.95(8)	74.47(8)	74.21(7)
O1–Mo–O2	98.55(8)	107.21(7)	107.53(7)	167.26(6)
O1–Mo–N2	97.21(9)	99.00(8)	99.04(8)	116.15(7)
O1–Mo–O	150.25(9)	142.45(9)	143.94(8)	
O1–Mo–O5				81.19(7)
O1–Mo–N6	77.77(8)	79.23(7)	80.66(8)	
O1–Mo–O6				89.59(7)
O2–Mo–N2	78.55(9)	77.18(8)	77.14(8)	74.99(7)
O2–Mo–N1	160.56(8)	161.80(8)	162.71(8)	115.03(7)
O2–Mo–O	104.48(9)	98.35(8)	98.30(8)	
O2–Mo–O5				92.04(7)
O2–Mo–N6	78.52(8)	77.39(8)	77.96(8)	
O2–Mo–O6				81.88(7)
N1–Mo–N2	84.34(9)	84.63(9)	85.58(8)	81.82(8)
N1–Mo–O	88.89(9)	89.22(9)	88.26(9)	
N1–Mo–O5				150.48(8)
N1–Mo–N6	116.50(9)	120.40(9)	119.04(8)	
N1–Mo–O6				90.12(8)
N2–Mo–O	105.54(9)	113.42(9)	111.14(9)	
N2–Mo–O5				94.94(7)
N2–Mo–N6	155.48(9)	152.68(9)	153.74(9)	
N2–Mo–O6				149.27(8)
O–Mo–N6	88.53(9)	80.08(8)	80.62(8)	
O5–Mo–O6				105.96(7)
Mo1–N5–Mo2		109.49(10)		
Mo1–N6–Mo2		89.79(8)		
Mo–O5–C52				136.25(15)
Mo–O6–C62				130.37(15)

^aFor (^tBuClip)₂Mo₂(μ-N)(μ-NH₂), N5 is analogous to O in (^tBuClip)MoO(lut). ^bAtom labels are those in (^tBuClip)MoO(lut) and Mo1 in (^tBuClip)₂Mo₂(μ-N)(μ-NH₂). For Mo2, the analogous atom labels are O3=O1, O4=O2, N3=N1, N4=N2.

by each molybdenum center in (^tBuClip)Mo(μ-N)(μ-NH₂)Mo(^tBuClip), with the oxo group in place of the bridging nitride and the lutidine in place of the bridging amide (Table 2). In particular, the oxo complex also shows a short metal–ligand multiple bond ($d_{\text{Mo}=\text{O}} = 1.7098(19)$ Å, consistent with a molybdenum–oxygen triple bond³⁰) and substantial distortion toward a trigonal prism (twist angles = $37 \pm 7^\circ$).

The observed solid-state geometry, *cis*-β with amidophenolate oxygen trans to oxo, is analogous to that observed in the nitride complex. In solution, this geometry appears to be strongly favored as well, but traces (~3%) of a minor isomer are observed. DFT calculations on (Clip)MoO(py) indicate that all three *cis* isomers are local minima, but the crystallographically observed isomer is strongly favored, with the *cis*-α geometry calculated to be 5.4 kcal/mol higher in energy and the other *cis*-β geometry (with amide trans to

oxo) 12 kcal/mol higher in energy (Figure 4). The observed *cis*-β geometry maximizes π bonding to the molybdenum. The amidophenoxide ligand trans to the oxo donates primarily into the Mo dπ orbital which does not interact with the oxo ligand, and overlap with this orbital is expected to be maximized if it is the amidophenoxide nitrogen that is *cis* to the oxo, since the amidophenoxide highest occupied molecular orbital (HOMO) has more density on nitrogen than oxygen and overlap with the dπ orbital is greater with the atom in this position (Figure 5b). The amidophenoxide with both donors *cis* to the oxo must compete with the oxo for π bonding to molybdenum. Calculations show a substantial difference in energy between the two amidophenoxide π-donor orbitals (Figure 5). Electrochemically (Supporting Information, Figure S2b), a reversible oxidation is observed at +0.06 V, with no other oxidations below +1.1 V.

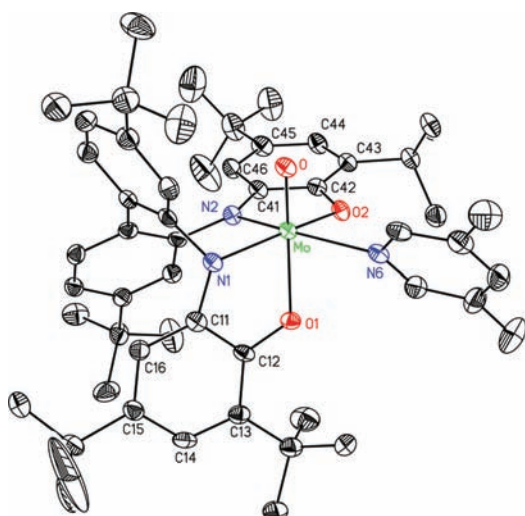


Figure 3. Thermal ellipsoid plot of $(^t\text{BuClip})\text{MoO}(\text{lut})\cdot\text{CH}_3\text{CN}$. Hydrogen atoms and solvent molecules are omitted for clarity.

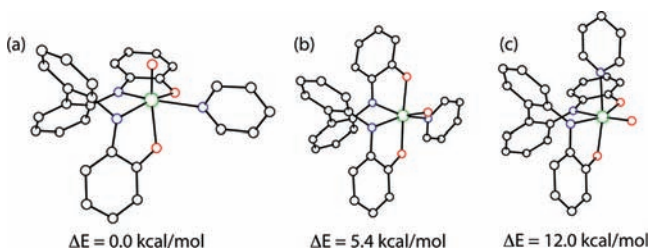


Figure 4. Calculated structures and relative energies (B3LYP, SDD (Mo)/6-31G*) of $(\text{Clip})\text{MoO}(\text{py})$ isomers: (a) *cis*- β , aryloxide trans to oxo; (b) *cis*- α ; (c) *cis*- β , amide trans to oxo.

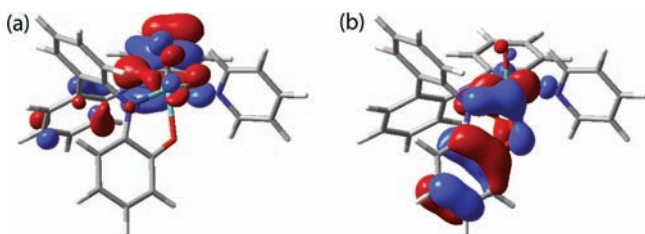
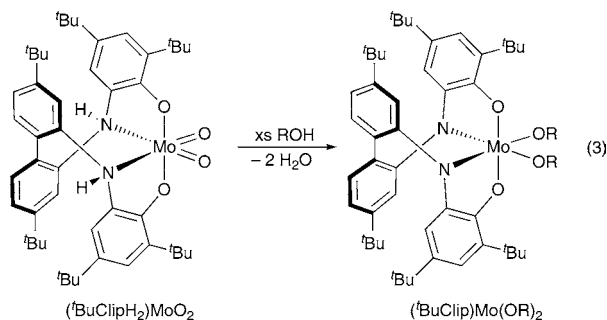


Figure 5. Kohn-Sham orbitals in $(\text{Clip})\text{MoO}(\text{py})$ (observed geometry). (a) HOMO, π -donor orbital from *cis* amidophenolate, $E = -4.79$ eV. (b) HOMO-1, π -donor orbital from *trans* amidophenolate, $E = -5.54$ eV.

When $(^t\text{BuClipH}_2)\text{MoO}_2$ is treated with excess methanol or isopropanol, both oxo ligands are lost and bis(alkoxide) complexes $(^t\text{BuClip})\text{Mo}(\text{OR})_2$ are formed (eq 3).



This is similar to the behavior exhibited by the oxo-bridged bis(catecholate) complex $\{(3,6\text{-}^t\text{Bu}_2\text{C}_6\text{H}_2\text{O}_2)_2\text{Mo}(\mu\text{-O})\}_4$.⁶

While in situ NMR spectroscopy indicates that yields of the bis(alkoxide) are high, material isolated from this reaction is usually contaminated with oxo-containing species, presumably resulting from the hydrolysis equilibrium shifting as the solutions are concentrated. (Addition of water to isolated $(^t\text{BuClip})\text{Mo}(\text{OR})_2$, in the absence of excess alcohol, causes hydrolysis to $(^t\text{BuClipH}_2)\text{MoO}_2$.) Thus, preparations of the alkoxides are most conveniently carried out starting with the nitrido complex $(^t\text{BuClip})\text{Mo}(\mu\text{-N})(\mu\text{-NH}_2)\text{Mo}(^t\text{BuClip})$, which also reacts with alcohols to form the bis(alkoxide) complexes. NMR spectra of $(^t\text{BuClip})\text{Mo}(\text{OR})_2$ are indicative of C_2 symmetry, and the ^1H NMR spectrum of the methoxide complex is unchanged down to -60 °C, suggesting a *cis*- α geometry for these compounds.

The *cis*- α geometry is confirmed by the solid-state structure of $(^t\text{BuClip})\text{Mo}(\text{O}^i\text{Pr})_2$ (Figure 6). In the solid state, there are

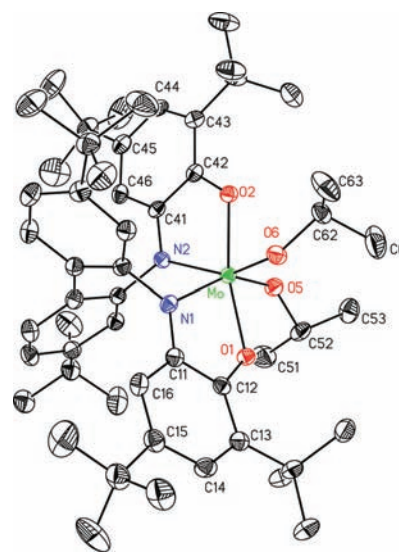


Figure 6. Thermal ellipsoid plot of $(^t\text{BuClip})\text{Mo}(\text{O}^i\text{Pr})_2\cdot 2\text{CH}_3\text{CN}$, with solvent molecules and hydrogen atoms omitted for clarity.

noticeable differences in the conformations of the two isopropoxide groups (especially the O5-Mo-O6-C62 and O6-Mo-O5-C52 dihedral angles, which are 50.0° and 91.4° , respectively) and small but statistically significant differences (~ 0.02 Å) among the pairs of analogous metal-ligand distances (Table 2), which lower the symmetry from the C_2 symmetry displayed in solution.

Pyridine Exchange in Monooxomolybdenum(VI) Complexes. ^1H NMR spectra of $(^t\text{BuClip})\text{MoO}(\text{L})$ ($\text{L} =$ pyridine, 3,5-lutidine) at room temperature in the presence of excess neutral ligand show broadened, but distinct, resonances characteristic of free and bound ligand, indicating that ligand exchange is taking place on the NMR time scale. Consistent with this explanation, reversible temperature-dependent changes are observed in the NMR (Figure 7), which can be analyzed quantitatively to extract the pyridine exchange rate. The linewidths of the bound pyridine signals in the slow-exchange regime are independent of the concentration of added pyridine, indicating that the exchange is zeroth-order in pyridine and hence dissociative. A dissociative reaction is also consistent with the observed activation parameters, in particular the positive entropies of activation ($\Delta H^\ddagger = 17.2(7)$ kcal/mol, $\Delta S^\ddagger = +9(2)$ cal/mol K for pyridine exchange, $\Delta H^\ddagger = 20.9(6)$ kcal/mol, $\Delta S^\ddagger = +17(2)$ cal/mol K for 3,5-lutidine exchange, Supporting

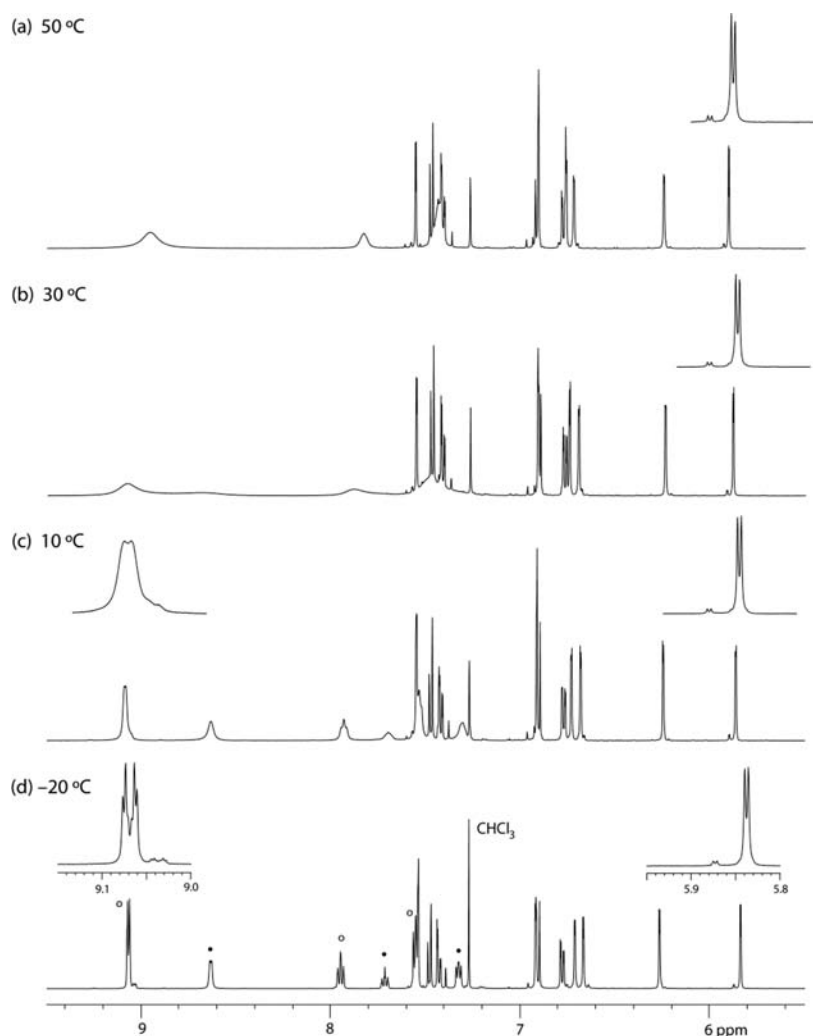
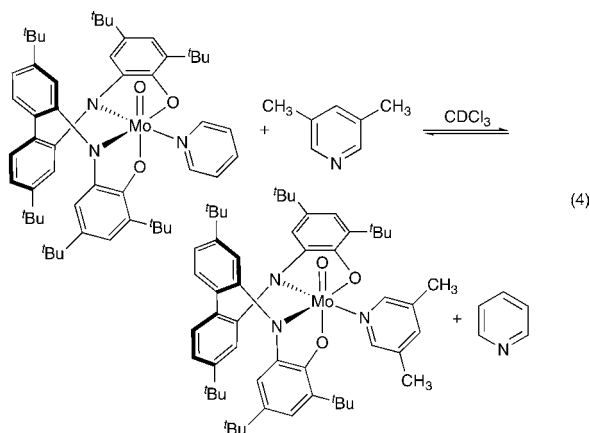


Figure 7. ^1H NMR spectra of $(^t\text{BuClip})\text{MoO}(\text{py})$ in the presence of excess pyridine (500 MHz, CDCl_3). (a) 50 °C; (b) 30 °C; (c) 10 °C; (d) -20 °C. Peaks due to bound pyridine (O) and free pyridine (●) are marked on the low-temperature spectrum. Insets: left, δ 9.00–9.15 ppm; right, 5.80–5.95 ppm.

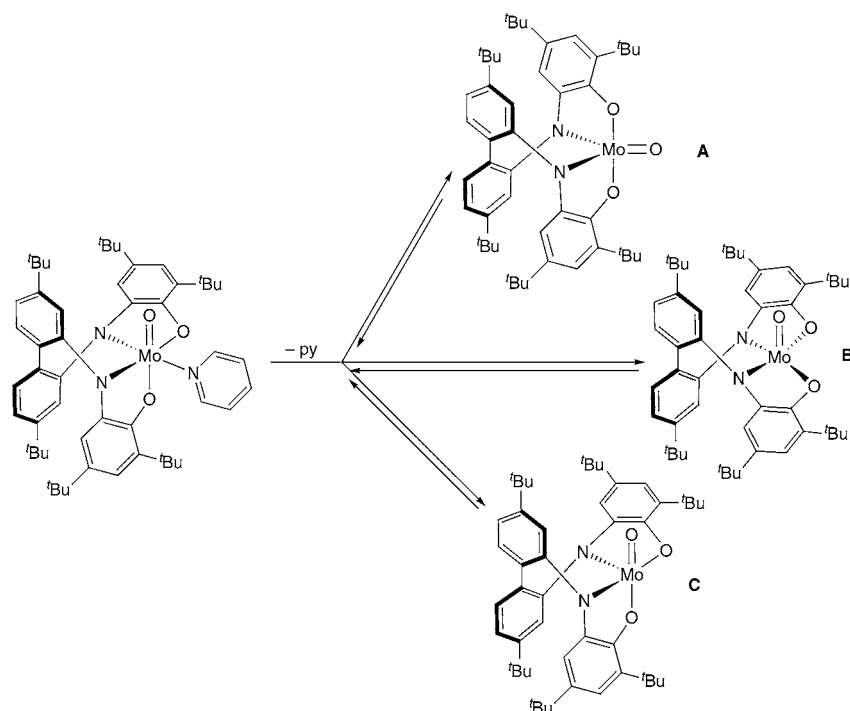
Information, Figure S3). The ~ 5 -fold slower rate for lutidine exchange is consistent with its greater basicity leading to tighter binding and hence slower dissociation. The stronger binding of lutidine was confirmed by measurement of the equilibrium constants for pyridine/lutidine exchange (eq 4) from -50 to +20 °C; van't Hoff analysis gives $\Delta H^\circ = -0.70 \pm 0.17$ kcal/mol, $\Delta S^\circ = -0.2 \pm 0.7$ cal/mol K (Supporting Information, Figure S4).



The resonances due to the 10 inequivalent aromatic protons and the 6 inequivalent ^tBu peaks in $(^t\text{BuClip})\text{MoO}(\text{L})$ do not

undergo broadening or exchange concurrently with the observed dissociation of the bound ligand. This rules out formation of a C_2 -symmetric, trigonal bipyramidal intermediate such as structure **A** (Scheme 2). The apparent stereochemical rigidity of the dissociated intermediate is somewhat surprising, given the propensity of d^0 complexes, especially those with small bite angle chelates, to undergo fluxional processes.³¹ In principle, relaxation of the five-coordinate intermediate to a quasi-symmetric structure such as square pyramidal **B** would be consistent with the observed stereochemical rigidity. The chirality of the biphenyl backbone discriminates between the two sides of the $^t\text{BuClip}$ ligand in **B**, and the twist of the biphenyl only allows one side of the ligand to resume its position trans to the oxo upon readdition of pyridine. (Chelating biphenoxide ligands similar to the 2,2'-diamidobiphenyl moiety have been observed to undergo racemization along their chiral axes, but the barriers are typically ~ 14 kcal/mol,^{32,33} indicating that twisting of the biphenyl moiety in **B** would likely be too slow to compete with pyridine rebinding.) However, the behavior of the minor isomer argues against this possibility. The bound pyridine in the minor isomer (left inset, Figure 7) undergoes exchange with free pyridine at a rate comparable to that shown by the major isomer, while the $^t\text{BuClip}$ backbone peaks (e.g., right inset, Figure 7) of the major and minor isomers remain sharp

Scheme 2. Possible Structures of the Five-Coordinate Intermediate Formed by Dissociation of Pyridine from $({}^t\text{BuClip})\text{MoO}(\text{py})$



and distinct over the entire temperature range studied. Since **B** is the only possible square pyramidal structure with an apical oxo, its formation would allow interconversion of the isomers, and thus it is unlikely to be on the pathway for pyridine exchange. The most likely explanation for the observed behavior is that dissociation of pyridine takes place to form a stereochemically rigid five-coordinate species, effectively a square pyramid with an equatorial oxo (e.g., **C** in Scheme 2).

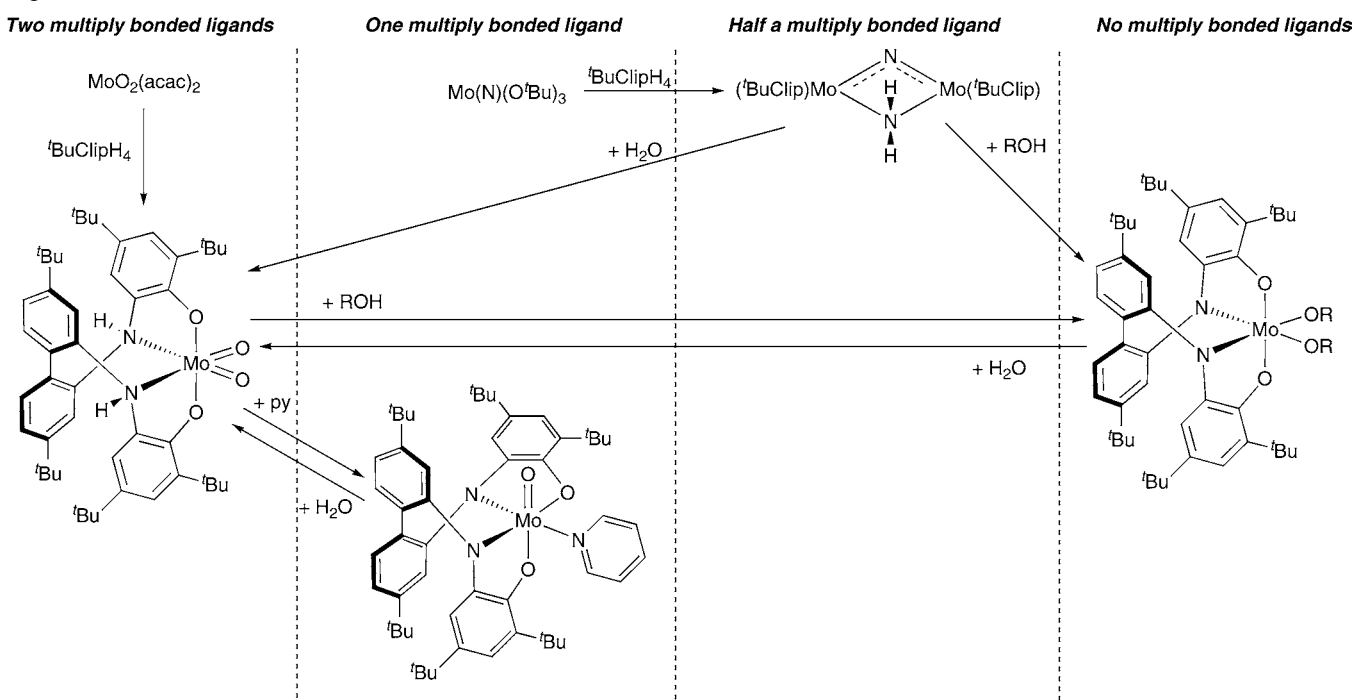
DISCUSSION

Molybdenum-Amidophenoxide π Bonding as a Driver of Structure and Reactivity. Molybdenum-amidophenoxide π bonding exerts a powerful influence on many aspects of the structure and reactivity of the $({}^t\text{BuClip})\text{Mo}$ complexes. The effects seen include the following.

Stabilization of Complexes without Other Metal–Ligand Multiple Bonds. In contrast to the usual high affinity of molybdenum(VI) for multiply bonded ligands, ${}^t\text{BuClip}$ -ligated molybdenum(VI) shows a remarkable indifference to the number of multiply bonded groups. Compounds containing two, one, or zero oxo ligands interconvert under mild conditions (Scheme 3). Formation of $({}^t\text{BuClip})\text{Mo}(\mu\text{-N})(\mu\text{-NH}_2)\text{-Mo}({}^t\text{BuClip})$ from ${}^t\text{BuClipH}_4$ and $\text{Mo}(\text{N})(\text{O}{}^t\text{Bu})_3$ also involves a diminution in the number of multiply bonded ligands, with two terminal nitrides being converted to a σ -only bridging amide and a highly bent μ -nitride capable of forming only one π bond among two molybdenums, making it effectively half of a multiply bonded ligand. The structural plasticity of the $({}^t\text{BuClip})\text{Mo}$ compounds parallels that shown by the isoelectronic bis(catecholate)molybdenum fragment $(3,6\text{-}{}^t\text{Bu}_2\text{C}_6\text{H}_2\text{O}_2)_2\text{Mo}$ described by Pierpont and co-workers.⁶ The bis(catecholate) complexes also readily form mono-oxo complexes as well as complexes lacking terminal oxo groups, such as the μ -oxo tetramer $\{(3,6\text{-}{}^t\text{Bu}_2\text{C}_6\text{H}_2\text{O}_2)_2\text{Mo}(\mu\text{-O})\}_4$ and the bis(alkoxide) $(3,6\text{-}{}^t\text{Bu}_2\text{C}_6\text{H}_2\text{O}_2)_2\text{Mo}(\text{O}{}^i\text{Pr})_2$.

Spectroscopic, Structural, and Dynamic Effects. Despite the parallels between the amidophenoxide and the catecholate ligand, a number of observations indicate that the former is a stronger donor than the latter. The amidophenoxide complexes $({}^t\text{BuClip})\text{MoO}(\text{L})$ show lower-frequency $\text{Mo}=\text{O}$ stretches ($901\text{--}907\text{ cm}^{-1}$) than do $(3,6\text{-}{}^t\text{Bu}_2\text{C}_6\text{H}_2\text{O}_2)_2\text{MoO}(\text{L})$ ($916\text{--}929\text{ cm}^{-1}$).⁶ The oxo-amidophenoxide complexes $({}^t\text{BuClip})\text{-MoO}(\text{L})$ also show enhanced lability of the neutral donors in comparison to their catecholate analogues. No exchange is observed between free and bound Me_2SO resonances in the oxo-dimethyl sulfoxide complex $(3,6\text{-}{}^t\text{Bu}_2\text{C}_6\text{H}_2\text{O}_2)_2\text{MoO}(\text{OSMe}_2)$ even at ambient temperatures.⁶ In contrast, $({}^t\text{BuClip})\text{MoO}(\text{py})$ shows facile dissociative loss of pyridine ($k_{\text{diss}} = 79\text{ s}^{-1}$, $\Delta G^\ddagger = 14.5\text{ kcal/mol}$ at $22\text{ }^\circ\text{C}$). Both of these traits indicate that the amidophenoxide is a stronger donor than catecholate, but do not distinguish between σ - and π -donating ability. However, the longer $\text{Mo}\text{--}\text{O}{}^i\text{Pr}$ distances in $({}^t\text{BuClip})\text{Mo}(\text{O}{}^i\text{Pr})_2$ (1.895 \AA vs 1.848 \AA) and more acute $\text{Mo}\text{--}\text{O}\text{--}\text{C}$ angles of the alkoxides (133° vs 143.35°) compared to $(3,6\text{-}{}^t\text{Bu}_2\text{C}_6\text{H}_2\text{O}_2)_2\text{Mo}(\text{O}{}^i\text{Pr})_2$ ⁶ speak more directly to the relative π -donor abilities of the chelating ligands compared to the alkoxides,³⁴ indicating that the greater donation from the amidophenoxides has a significant π component.

Stereochemical Effects. The stereochemistry of $({}^t\text{BuClip})\text{-Mo}(\mu\text{-N})(\mu\text{-NH}_2)\text{Mo}({}^t\text{BuClip})$ and of $({}^t\text{BuClip})\text{MoO}(\text{lut})$ can be rationalized on the basis of the π -bonding predilections of the amidophenoxide ligand. The amidophenoxide is aligned so that it can donate into $d\pi$ orbitals not involved in π -bonding with the multiply bonded ligands, and is in an orientation that maximizes overlap of this $d\pi$ orbital with the nitrogen of the amidophenoxide, which contributes more to the ligand's π -donor orbital than the oxygen. It could be argued that this orientation is merely the result of the trans influence of the oxo or nitrido ligand, which will favor placing the strongly donating amide in the cis position. The behavior of the isoelectronic

Scheme 3. Interconversions between (^tBuClip)Mo Complexes with Different Numbers of Multiply Bonded Oxo or Nitrido Ligands

oxobis(catecholate) complexes, however, clearly indicates the greater influence of π bonding over the trans influence. In these compounds, the trans influence would strongly favor placing the neutral donor trans to the oxo, but it is the cis complex that is observed. (The same argument could be made for the ^tBuClip complexes but is complicated by the geometrical constraints of the biphenyl bridge, which would create significant distortions in a trans geometry.¹⁷) Indeed, the observed stereodynamics of (3,6-^tBu₂C₆H₂O₂)₂MoO(OSMe₂)⁶ indicates that the trans geometry is not even readily accessible as an intermediate. The complex undergoes facile trigonal twists on the NMR time scale, with the onset of broadening due to Bailar twisting below $-98\text{ }^{\circ}\text{C}$ ($\Delta G^{\ddagger} < 9.5\text{ kcal/mol}^{35}$), but this process does not exchange all the aromatic hydrogen environments and therefore cannot involve formation of the trans isomer. Full exchange among all four aromatic hydrogen environments is observed at about $-30\text{ }^{\circ}\text{C}$ ($\Delta G^{\ddagger} \approx 13.5\text{ kcal/mol}$),³⁶ but Ray–Dutt twists could accomplish this exchange even without formation of the trans isomer, suggesting that the trans isomer is disfavored by at least this much energy.

In addition to their ability to engage in π bonding, amidophenoxides are well-known “noninnocent” ligands capable of existing in oxidized (iminoquinone or iminoquinone) forms.³⁷ An analogue of the ^tBuClip ligand has been observed to form bis(iminoquinone) complexes with Cu, Pd, and Pt.¹⁷ Formulating any of the compounds described here as (iminoquinone)-Mo(V) complexes, however, does not appear to be appropriate. All of the complexes described here are diamagnetic, and molybdenum(VI) with strong π donor ligands is not especially oxidizing. Furthermore, the geometrical features of the complexes are accurately described by single-determinant, closed-shell singlet DFT calculations, indicating that a more complex view of the electronic structure of the complexes need not be invoked. A careful inspection of the metrical data in the three structures does reveal geometric distortions similar to those seen in complexes with oxidized ligands, but a detailed analysis of these

distortions³⁸ suggests that they, too, are a symptom of strong π donation rather than ligand oxidation.

CONCLUSIONS

The 2,2'-biphenyl-bridged bis(aminophenol) ligand ^tBuClipH₄ forms high-valent molybdenum complexes with variable numbers of multiply bonded ancillary ligands. In its doubly deprotonated state, the ligand forms the cis-dioxo complex (^tBuClipH₂)MoO₂. When fully deprotonated, it forms monometallic complexes with one terminal oxo ligand, the bimetallic complex (^tBuClip)Mo(μ -N)(μ -NH₂)Mo(^tBuClip) where two molybdenum atoms share a nitrido ligand, and oxo- and nitrido-free bis(alkoxide) complexes (^tBuClip)Mo(OR)₂. The facile formation and interconversion of these species underscores the ability of the amidophenoxide ligand to stabilize molybdenum(VI) through strong π -donation, as does the facile loss of pyridine from (^tBuClip)MoO(py) to form a stereochemically rigid five-coordinate intermediate.

ASSOCIATED CONTENT

Supporting Information

Crystallographic information on (^tBuClip)Mo(μ -N)(μ -NH₂)-(^tBuClip)-0.5Et₂O, (^tBuClip)MoO(3,5-lutidine)·CH₃CN, and (^tBuClip)Mo(O^tPr)₂·2CH₃CN in CIF format; details of calculations, electrochemistry, and variable-temperature NMR (PDF format). This material is available free of charge via the Internet at <http://pubs.acs.org>.

AUTHOR INFORMATION

Corresponding Author

*E-mail: Seth.N.Brown.114@nd.edu.

ACKNOWLEDGMENTS

We thank Dr. Mauricio Quiroz-Guzman and Dr. Allen Oliver for their assistance with the X-ray crystallography. This work was supported by a grant from the Notre Dame Sustainable

Energy Initiative and by the donors of the Petroleum Research Fund, administered by the American Chemical Society. J.A.K. gratefully acknowledges the support of a Vincent Slatt Research Fellowship in Energy Systems and of a Summer Undergraduate Research Fellowship from the Notre Dame College of Science.

REFERENCES

- (1) Holm, R. H.; Donahue, J. P. *Polyhedron* **1993**, *12*, 571–589.
- (2) Young, C. G. In *Comprehensive Coordination Chemistry II*; McCleverty, J. A., Meyer, T. J., Eds.; Elsevier: New York, 2003; Vol. 4, pp 415–527.
- (3) (a) Gordon, D. J.; Fenske, R. F. *Inorg. Chem.* **1982**, *21*, 2907–2915. (b) Dulatas, L. T.; Brown, S. N.; Ojomo, E.; Noll, B. C.; Cavo, M. J.; Holt, P. B.; Wopperer, M. M. *Inorg. Chem.* **2009**, *48*, 10789–10799.
- (4) (a) Pierpont, C. G.; Downs, H. H. *J. Am. Chem. Soc.* **1975**, *97*, 2123–2127. (b) Pierpont, C. G.; Buchanan, R. M. *J. Am. Chem. Soc.* **1975**, *97*, 4912–4917. (c) Cass, M. E.; Pierpont, C. G. *Inorg. Chem.* **1986**, *25*, 122–123.
- (5) Buchanan, R. M.; Pierpont, C. G. *Inorg. Chem.* **1979**, *18*, 1616–1620.
- (6) Liu, C.-M.; Nordlander, E.; Schmeh, D.; Shoemaker, R.; Pierpont, C. G. *Inorg. Chem.* **2004**, *43*, 2114–2124.
- (7) (a) Wilshire, J. P.; Leon, L.; Bosserman, P.; Sawyer, D. T. *J. Am. Chem. Soc.* **1979**, *101*, 3379–3381. (b) Lim, M.-C.; Sawyer, D. T. *Inorg. Chem.* **1982**, *21*, 2839–2841. (c) Bristow, S.; Enemark, J. H.; Garner, C. D.; Minelli, M.; Morris, G. A.; Ortega, R. B. *Inorg. Chem.* **1985**, *24*, 4070–4077. (d) Bristow, S.; Garner, C. D.; Morris, G. A.; Enemark, J. H.; Minelli, M.; Ortega, R. B. *Polyhedron* **1986**, *5*, 319–321. (e) Bradbury, J. R.; Schultz, F. A. *Inorg. Chem.* **1986**, *25*, 4416–4422. (f) Liu, S.; Shaikh, S. N.; Zubieta, J. *Inorg. Chem.* **1987**, *26*, 4303–4305. (g) Gheller, S. F.; Newton, W. E.; Pabon de Majid, L.; Bradbury, J. R.; Schultz, F. A. *Inorg. Chem.* **1988**, *27*, 359–366. (h) Mondal, J. U.; Schultz, F. A.; Brennan, T. D.; Scheidt, W. R. *Inorg. Chem.* **1988**, *27*, 3950–3956. (i) Kumar, S. B.; Chaudhury, M. J. *Chem. Soc., Dalton Trans.* **1991**, 2169–2174. (j) Albrecht, M.; Franklin, S. J.; Raymond, K. N. *Inorg. Chem.* **1994**, *33*, 5785–5793. (k) Reibenspies, J. H.; Klausmeyer, K.; Darensbourg, D. Z. *Kristallogr.* **1994**, *209*, 761–762. (l) Duhme, A.-K.; Davies, S. C.; Hughes, D. L. *Inorg. Chem.* **1998**, *37*, 5380–5382. (m) Mondal, J. U.; Zamora, J. G.; Kinon, M. D.; Schultz, F. A. *Inorg. Chim. Acta* **2000**, *309*, 147–150. (n) Mondal, J. U.; Zamora, J. G.; Siew, S.-C.; Garcia, G. T.; George, E. R.; Kinon, M. D.; Schultz, F. A. *Inorg. Chim. Acta* **2001**, *321*, 83–88. (o) Mondal, J. U.; Almaraz, E.; Bhat, N. G. *Inorg. Chem. Commun.* **2004**, *7*, 1195–1197. (p) Albrecht, M.; Baumert, M.; Klankermayer, J.; Kogej, M.; Schalley, C. A.; Fröhlich, R. *Dalton Trans.* **2006**, 4395–4400. (q) Monteiro, B.; Cunha-Silva, L.; Gago, S.; Klinowski, J.; Paz, F. A. A.; Rocha, J.; Gonçalves, I. S.; Pillinger, M. *Polyhedron* **2010**, *29*, 719–730.
- (8) Carter, S. M.; Sia, A.; Shaw, M. J.; Heyduk, A. F. *J. Am. Chem. Soc.* **2008**, *130*, 5838–5839.
- (9) Tashiro, M.; Yamato, T. *J. Org. Chem.* **1979**, *44*, 3037–3041.
- (10) Chan, D. M.-T.; Chisholm, M. H.; Folting, K.; Huffman, J. C.; Marchant, N. S. *Inorg. Chem.* **1986**, *25*, 4170–4174.
- (11) Connelly, N. G.; Geiger, W. E. *Chem. Rev.* **1996**, *96*, 877–910.
- (12) Lionetti, D.; Medvecz, A. J.; Ugrinova, V.; Quiroz-Guzman, M.; Noll, B. C.; Brown, S. N. *Inorg. Chem.* **2010**, *49*, 4687–4697.
- (13) Frisch, M. J.; Trucks, G. W.; Schlegel, H. B.; Scuseria, G. E.; Robb, M. A.; Cheeseman, J. R.; Montgomery, J. A.; Vreven, T.; Kudin, K. N.; Burant, J. C.; Millam, J. M.; Iyengar, S. S.; Tomasi, J.; Barone, V.; Mennucci, B.; Cossi, M.; Scalmani, G.; Rega, N.; Petersson, G. A.; Nakatsuji, H.; Hada, M.; Ehara, M.; Toyota, K.; Fukuda, R.; Hasegawa, J.; Ishida, M.; Nakajima, T.; Honda, Y.; Kitao, O.; Nakai, H.; Klene, M.; Li, X.; Knox, J. E.; Hratchian, H. P.; Corss, J. B.; Adamo, C.; Jaramillo, J.; Gomperts, R.; Stratmann, R. E.; Yazyev, O.; Austin, A. J.; Cammi, R.; Pomelli, C.; Ochterski, J. W.; Ayala, P. Y.; Morokuma, K.; Voth, G. A.; Salvador, P.; Dannenberg, J. J.; Zakrzewski, V. G.; Dapprich, S.; Daniels, A. D.; Strain, M. C.; Farkas, O.; Malick, D. K.; Rabuck, A. D.; Raghavachari, K.; Foresman, J. B.; Ortiz, J. V.; Cui, Q.; Baboul, A. G.; Clifford, S.; Cioslowski, J.; Stefanov, B. B.; Liu, G.; Liashenko, A.; Piskorz, P.; Komaromi, I.; Martin, R. L.; Fox, D. J.; Keith, T.; Al-Laham, M. A.; Peng, C. Y.; Nanayakkara, A.; Challacombe, M.; Gill, P. M. W.; Johnson, B.; Chen, W.; Wong, M. W.; Gonzalez, C.; Pople, J. A. *Gaussian 03*, Revision C.01; Gaussian Inc.: Wallingford, CT, 2004.
- (14) Budzelaar, P. H. M. *gNMR*, v. 3.5.6; Cherwell Scientific Publishing: Oxford, U.K., 1996.
- (15) Sheldrick, G. M. *Acta Crystallogr., Sect. A* **2008**, *A64*, 112–122.
- (16) *International Tables for Crystallography*; Kluwer Academic Publishers: Dordrecht, The Netherlands, 1992; Vol. C.
- (17) Mukherjee, C.; Weyhermüller, T.; Bothe, E.; Chaudhuri, P. *Inorg. Chem.* **2008**, *47*, 11620–11632.
- (18) O'Shaughnessy, P. N.; Knight, P. D.; Morton, C.; Gillespie, K. M.; Scott, P. *Chem. Commun.* **2003**, 1770–1771.
- (19) Zelikoff, A. L.; Kopilov, J.; Goldberg, I.; Coates, G. W.; Kol, M. *Chem. Commun.* **2009**, 6804–6806.
- (20) Wentworth, R. A. D. *Coord. Chem. Rev.* **1972**, *9*, 171–187.
- (21) (a) Strähle, J. Z. *Anorg. Allg. Chem.* **1970**, *375*, 238–254. (b) Strähle, J.; Weiher, U.; Dehnicke, K. Z. *Naturforsch.* **1978**, *33B*, 1347–1351. (c) Müller, U.; Kujanek, R.; Dehnicke, K. Z. *Anorg. Allg. Chem.* **1982**, *495*, 127–134. (d) Dietrich, A.; Neumüller, B.; Dehnicke, K. Z. *Anorg. Allg. Chem.* **1999**, *625*, 1589–1591. (e) Gauch, E.; Hagenbach, A.; Strähle, J.; Dietrich, A.; Neumüller, B.; Dehnicke, K. Z. *Anorg. Allg. Chem.* **2000**, *626*, 489–493.
- (22) Bishop, M. W.; Chatt, J.; Dilworth, J. R. *J. Chem. Soc., Chem. Commun.* **1976**, 780–781.
- (23) (a) Kim, G.-S.; DeKock, C. W. *Chem. Commun.* **1989**, 1166–1168. (b) Herrmann, W. A.; Bogdanovic, S.; Priemeier, T.; Poli, R.; Fettinger, J. C. *Angew. Chem., Int. Ed.* **1995**, 112–115.
- (24) (a) Godemeyer, T.; Weller, F.; Dehnicke, K.; Fenske, D. Z. *Anorg. Allg. Chem.* **1987**, *554*, 92–100. (b) Figge, R.; Friebel, C.; Patt-Siebel, U.; Müller, U.; Dehnicke, K. Z. *Naturforsch.* **1989**, *44B*, 1377–1384. (c) Hughes, D. L.; Mohammed, M. Y.; Pickett, C. J. *J. Chem. Soc., Dalton Trans.* **1990**, 2013–2019. (d) Debad, J. D.; Legzdins, P.; Reina, R.; Young, M. A.; Batchelor, R. J.; Einstein, F. W. B. *Organometallics* **1994**, *13*, 4315–4321. (e) Agapie, T.; Odom, A. L.; Cummins, C. C. *Inorg. Chem.* **2000**, *39*, 174–179.
- (25) (a) Noble, M. E.; Folting, K.; Huffman, J. C.; Wentworth, R. A. D. *Inorg. Chem.* **1982**, *21*, 3772–3776. (b) Johnson, M. J. A.; Lee, P. M.; Odom, A. L.; Davis, W. M.; Cummins, C. C. *Angew. Chem., Int. Ed. Engl.* **1997**, *36*, 87–91. (c) Solari, E.; Da Silva, C.; Iacono, B.; Hesschenbrouck, J.; Rizzoli, C.; Scopelliti, R.; Floriani, C. *Angew. Chem., Int. Ed.* **2001**, *40*, 3907–3909. (d) Gibson, V. C.; Williams, D. N.; Clegg, W. *Chem. Commun.* **1989**, 1863–1864. (e) Tsai, Y.-C.; Johnson, M. J. A.; Mindiola, D. J.; Cummins, C. C.; Klooster, W. T.; Koetzle, T. F. *J. Am. Chem. Soc.* **1999**, *121*, 10426–10427. (f) Du, Y.; Rheingold, A. L.; Maatta, E. A. *J. Chem. Soc., Chem. Commun.* **1994**, 2163–2164.
- (26) (a) Pollagi, T. P.; Manna, J.; Geib, S. J.; Hopkins, M. D. *Inorg. Chim. Acta* **1996**, *243*, 177–183. (b) Tonzetich, Z. J.; Schrock, R. R.; Wampler, K. M.; Bailey, B. C.; Cummins, C. C.; Müller, P. *Inorg. Chem.* **2008**, *47*, 1560–1567.
- (27) Woodman, P. R.; Munslow, I. J.; Hitchcock, P. B.; Scott, P. *J. Chem. Soc., Dalton Trans.* **1999**, 4069–4076.
- (28) (a) Ugrinova, V.; Noll, B. C.; Brown, S. N. *Inorg. Chem.* **2006**, *45*, 10309–10320. (b) Kongprakaiwoot, N.; Armstrong, J. B.; Noll, B. C.; Brown, S. N. *Dalton Trans.* **2010**, 39, 10105–10115.
- (29) Scott, A. P.; Radom, L. *J. Phys. Chem.* **1996**, *100*, 16502–16513.
- (30) Mayer, J. M. *Inorg. Chem.* **1988**, *27*, 3899–3903.
- (31) Fortner, K. C.; Bigi, J. P.; Brown, S. N. *Inorg. Chem.* **2005**, *44*, 2803–2814.
- (32) Pastor, S. D.; Carinci, A.; Khoury, N.; Rahni, D. N. *Inorg. Chem.* **2001**, *40*, 3830–3832.
- (33) Kongprakaiwoot, N.; Quiroz-Guzman, M.; Oliver, A. G.; Brown, S. N. *Chem. Sci.* **2011**, *2*, 331–336.
- (34) Smith, G. D.; Fanwick, P. E.; Rothwell, I. P. *Inorg. Chem.* **1990**, *29*, 3221–3226.

(35) Faller, J. W. In *Encyclopedia of Inorganic Chemistry*; King, R. B., Ed.; John Wiley and Sons: New York, 1994; pp 3914–3933.

(36) In ref 6, the authors note that the maintenance of an AB pattern in the aromatic region at $-30\text{ }^{\circ}\text{C}$ requires the operation of a Bailar, but not a Ray–Dutt, twist. However, the further coalescence of resonances above $-30\text{ }^{\circ}\text{C}$ requires the operation of a Ray–Dutt twist at these higher temperatures.

(37) Chun, H.; Chaudhuri, P.; Weyhermüller, T.; Wieghardt, K. *Inorg. Chem.* **2002**, *41*, 790–795.

(38) Brown, S. N. *Inorg. Chem.* **2012**, *51*, in press. DOI: 10.1021/ic202764j.